Canadian Conference - Pacific Conference on Earthquake Engineering 2023
Vancouver, British Columbia
June 25th – June 30th, 2023

Seismic Performance Enhancement of an Unstiffened Eight Bolt Extended End-Plate Moment Connection

Shahriar Quayyum[1*], Machel L. Morrison[2] and Tasnim Hassan[3]

[1]Assistant Professor, Department of Civil & Environmental Engineering, Manhattan College, Riverdale, NY 10471
[2]Assistant Professor, Department of Structural Engineering, University of California San Diego, La Jolla, CA 92093
[3]Professor, Department of Civil, Construction & Environmental Engineering, Raleigh, NC 27695
[*]shahriar.quayyum@manhattan.edu (Corresponding Author)

ABSTRACT

The eight-bolt stiffened extended end plate (8ES) connection is one of the connections prequalified for use in special and intermediate moment frames in ANSI/AISC 358. Simulated seismic testing of 8ES connections has generally shown sound performance with ductile failure modes. However, fast fracture of the beam flange at the stiffener toe has been observed in a recent study and was attributed to the high stress concentration in this region. To address this problem, an unstiffened eight-bolt extended end plate connection in which the stress concentration is eliminated by removing the stiffener, and the bolts are rearranged into an octagonal pattern to ensure uniform distribution of bolt forces, has been recently proposed. The study herein performed detailed finite element analyses to demonstrate that despite the improvements, high strain demands at the beam flange to end plate CJP welds may develop when the proposed unstiffened connection is used in conjunction with deep wide flange beam sections (e.g. W-sections of 900 mm nominal depth). Hence, two (2) additional seismic performance-enhancing techniques are analytically evaluated for unreinforced eight-bolt extended end plate connections. The first technique uses heat treatment of specified beam flange regions which relocates the plastic hinge and thereby lower flange weld strain demands. The second technique uses an extended heavy shear tab to relocate the plastic hinge away from flange weld and slightly delays the onset of strength degradation. Systematic analysis results are developed and presented to demonstrate the enhanced seismic resilience of the modified EEP connections and to plan future experimentations and design development.

Keywords: Extended end plate connection, seismic performance enhancement, octagonal bolt arrangement, extended end plate stiffener, heat-treated beam section, web reinforcement, extended shear tab.

INTRODUCTION

The construction of an extended end plate (EEP) connection involves shop welding a steel plate to one end of the beam which is then attached to the connecting members through bolts. The erection of EEP connections is faster than that of welded moment connections because of no need for field welding. Due in part to their economy and simplicity in fabrication and erection, EEP connections are widely used in European practice [1]. Furthermore, simulated seismic testing of EEP connections have shown that they can provide significant ductility and energy dissipation [2]. Therefore, EEP connections have been prequalified in the ANSI/AISC 358 [3] for use in special and intermediate moment frames in the U.S. Currently three (3) types of EEP connections are prequalified, the four-bolt unstiffened (4E), the four-bolt stiffened (4ES) and the eight-bolt stiffened (8ES). In 4ES and 8ES connections, the beam flange is stiffened by welding a stiffener plate between the beam flange and the end plate (Fig. 1a-b) in order to enhance the end plate's stiffness and strength, reducing prying forces and hence bolt force demands. Although in some studies these stiffened connections have shown ductile behavior, several studies have reported crack initiation at the stiffener toe leading to premature beam flange fractures [4-7]. It is to be noted here that in these studies the connections were not designed according to ANSI/AISC 358 [3]. However, in a relatively recent study [8] where the connections were designed according to ANSI/AISC 358 (2010), cracks in beam flange at the stiffener toe were noted in several 8ES connections and in one case, these cracks led to a brittle overload fracture during loading cycles at 4.7% interstory drift. This type of failure was explained as a consequence of the sharp change in the geometry of the connection at the stiffener toe which resulted in high stress concentration and triaxiality in this region [8]. Also, defects in the weld between the stiffener and beam flange, which may not be detected by welding inspection practice [9-10], may introduce additional sources of stress concentrations in this region.

Therefore, in order to alleviate these stress concentrations, an improved eight-bolt unstiffened extended end plate connection has recently been proposed based on comprehensive finite element analyses of EEP connections [11-12]. The proposed connection recommends removal of the end plate stiffener and rearranging the bolts into an octagonal pattern to facilitate uniform bolt force distribution [12]. It has been demonstrated through finite element analysis that the octagonal bolt pattern reduces stress concentrations at beam flanges, delays or reduces the strength degradation rate from local buckling and ensures more uniform bolt force distribution than those of alternative connections [12]. Moreover, removal of end plate stiffener in the proposed connection eliminates associated welding and fabrication costs which are anticipated to reduce the overall fabrication costs. In addition, the proposed connection offers the advantage of increased usable space on the floor because of the elimination of end plate stiffener. However, the proposed modified connection in [12] was studied for a W30×99 (W760×147)[1] beam section connected to a W14×193 (W360×287) column section. The feasibility of the proposed connection for heavier size beam sections is yet to be investigated.

In this study, the proposed eight-bolt EEP connection with octagonal bolt arrangement is investigated for heavier beam sections under simulated seismic loading by using finite element analysis. The analysis demonstrated that large stress and strain demands develop at the beam flange to end plate CJP welds for larger beam sections which motivated the introduction of a recently developed connection overstress mitigation technique [13]. This technique involves heat treating specific sections of the beam flanges with high temperatures which is then cooled slowly to room temperature. The heat-treatment reduces the strength of the steel and promotes plastic hinge formation at the heat-treated beam section (HBS) in a manner similar to the reduced beam section (RBS). Overall, there is a significant reduction in the strain demands at the weld between beam flange and end plate. An eight-bolt extended end plate connection modified with the octagonal bolt pattern and HBS eliminates the necessity of end plate stiffener and demonstrates potential applicability to a wide range of available beam sections. This modified eight-bolt EEP connection demonstrated strength degradation initiating as early as at 3% interstory drift. Although the proposed modified connection with heat treatment and web reinforcement delayed the onset of strength degradation to 5-6% interstory drift angle which is substantially higher than the required 4% interstory drift angle by ANSI/AISC 341 [14] for use in special moment frames, the introduction of heat treatment and web reinforcement requires a considerable effort and time for fabrication and entails additional expenses. Hence, as a design alternative, the modified connection with octagonal bolt arrangement is investigated with a heavy extended shear tab to study its seismic performances. The heavy extended shear tab reinforces the web region near the beam flange to end plate CJP weld and relocates the plastic hinge and thereby, reduces the strain demands on the beam flange CJP weld. However, the strength degradation is delayed slightly compared to the existing eight bolt moment connections, but satisfies the 4% interstory drift angle criteria as set forth by ANSI/AISC 341 [14] for use in special moment frames. The development of the proposed connections as design alternatives to the existing eight bolt extended end-plate connection along with the details of the finite element modeling is described below where each of the afore-mentioned performance enhancement techniques is clearly shown to have a pronounced effect on low-cycle fatigue failure resilience, plastic hinge formation, and strength degradation due to local buckling.

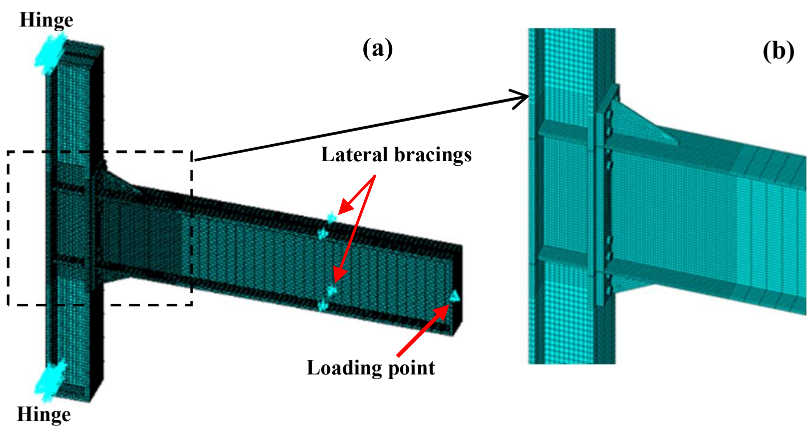

Figure 1. (a) Finite element mesh of an eight-bolt stiffened (8ES) extended end plate connection, (b) close up view of finite element mesh.

NUMERICAL SCHEME

Three-dimensional nonlinear finite element models were developed for extended end plate connections by using the general-purpose finite element analysis (FEA) software ANSYS. The finite element mesh and assumed boundary conditions for an eight-bolt stiffened extended end plate connection is presented in Figure 1. The top and bottom of the column flange nodes were considered hinged, lateral (roller) supports were provided to the beam flanges near the loading point and the free end of the beam was loaded with vertical displacements in accordance with the quasi-static cyclic SAC loading protocol [15]. A schematic of the loading protocol is shown in Figure 2. The finite element models include geometric, contact and material

[1] Metric units in parentheses

nonlinearities. The beams and columns were modeled and discretized by eight noded solid brick elements (SOLID 185). In order to precisely model the bolts and their interaction with the end plate, the end plate and the bolts were discretized by twenty noded solid brick elements (SOLID 186). Small sliding contact surfaces were defined between column flange and end plate, end plate and bolt head, column flange and bolt nut, bolt shank and circular holes in column flange and end plate. Surface-to-surface contact elements (CONTA 174) and target elements (TARGE 170) were used to generate the contact regions. Frictional contact was generated using the penalty method with a normal contact stiffness factor of 0.1 determined by using trial and error to minimize surface penetration and avoid numerical convergence issues. The coefficient of friction was taken as 0.35 for class A faying surfaces obtained from AISC LRFD Specification [16]. Pretension in the connecting bolts was modeled by using the PRETS179 pretension element which is used to define a pretension section within a meshed structure. PRETS179 element is defined by three nodes and the section data which define the pretension load direction relative to the pretension surface. Pretension loads were applied at the center of cross section of the bolt shank. The pretension load was applied as specified by the AISC LRFD Specification [16]. During simulations, first the bolt pretension was applied and associated displacement was stored. This displacement is used as an initial displacement during simulated seismic loading at the free end of the beam. Large deformation formulation was used to incorporate geometric nonlinearities. In the simulations, no initial imperfections were used to account for local buckling of the beam. During cyclic loading, it was noted that small eccentricities accumulate in the connection in spite of symmetric boundary conditions, loads and mesh. Because of the development of these small eccentricities during cyclic loading history, simulation of local buckling with reasonable accuracy was possible without introducing any initial imperfection. Similar observations have also been made in other studies [12, 17-18].

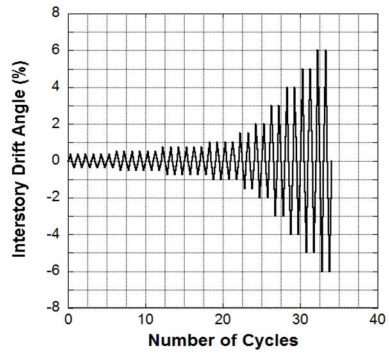

Figure 2. SAC loading protocol [15].

The constitutive model considered for steel was a rate-independent nonlinear kinematic hardening model proposed by Chaboche [19]. The constitutive equations are based on linear isotropic elasticity, a von-Mises yield function, associated flow rule and non-linear kinematic hardening rule. The model allows the superposition of several kinematic hardening rules and thus enables accurate simulation of hysteretic loop shape and thereby plastic modulus for a wide strain range. In the extended end plate connections studied, ASTM A992 and A572 Gr.50 steels were used for the beam and column material, whereas ASTM A36 was used for the end plate material. Bolts were modeled as ASTM A490 high strength bolts. Chaboche model parameters were determined by simulating stable hysteresis loops from strain-controlled experiments of ASTM A572 Gr.50 (data from [20]), ASTM A36 (data from [20]) and ASTM A992 (data from [13]) steels. The cyclic stress responses of ASTM A572 Gr.50, ASTM A36 and ASTM A992 steels do not change much with cycle (not shown) and hence, the stabilized hysteresis response was used to calibrate the kinematic hardening rule parameters, and no isotropic hardening rule was needed. The nonlinear kinematic hardening parameters for the steels used in this study are listed in Table 1. The material properties of ASTM A490 bolts were determined by performing uniaxial tests, and parameters for Chaboche model (shown in Table 1) were obtained by simulating the monotonic stress-strain curve. The weld metal between end plate and beam flanges was modeled using a bilinear kinematic hardening model using model parameters from FEMA-355B [9] (not shown).

Table 1. Nonlinear kinematic hardening parameters for different steels

Parameters	ASTM A36	ASTM A572 Gr.50	ASTM A992	ASTM A490	ASTM A992 (HBS)
E (MPa)	186861	191505	199948	199948	192122.5
σ_0 (MPa)	261.5	251.7	238.6	777.7	193.1
C_1 (MPa)	119996.4	125415.7	383336.8	204615.8	376789.7
C_2 (MPa)	10873.1	28868.4	280782.1	152250.1	262315.1
C_3 (MPa)	537.8	2675.2	50780	101318.5	60548.8
C_4 (MPa)	68.9	144.8	1958.3	32219.2	3232.8
γ_1	1036	4585	21081.2	4143	23485.9
γ_2	129	324	6256.2	285	20382.6
γ_3	5	42	515	107	552.5
γ_4	0	0	13.2	0	0

Validation of Finite Element Simulation Model

Finite element models of extended end plate moment connections were validated against the experimental responses of two eight-bolt stiffened (8ES-1.25-1.75-30 and 8ES-1.25-2.5-36)[2], two eight-bolt 4 wide unstiffened (8E-4W-1.25-1.125-30 and 8E-4W-1.25-1.375-36) extended end plate connections tested by Sumner *et al.* [21]. These connections consisted of a W30× 99 (W760×147) and W36× 150 (W920×223) (ASTM A572 Gr.50) beam sections attached to a W14× 193 (W360×287) and W14× 257 (W360×382) (ASTM A572 Gr.50) columns, respectively. Comparisons of the simulated and experimental moment-

[2]Specimen name includes: connection type-bolt diameter-end plate thickness-beam depth in inches

rotation responses of test specimens demonstrated that the hysteresis loop shapes and peak moments in each cycle are simulated with good accuracy as shown in Figure 3a for specimen 8ES-1.25-2.5-36. Moreover, simulated axial bolt strain responses matched reasonably well with the experimental responses for all the specimens. One such comparison is shown in Figure 3b. It is obsereved that the maximum axial bolt strains predicted by the finite element simulation are within 3% of the measured values. Nevertheless, it is noted that the gradual reduction in strain due to relaxtion is not well predicted by the simulation. In addition to force-displacement and bolt strain responses, plastic hinge formation and local buckling in the connection is also simulated with good accuracy (compare Figure 3c to 3d for specimen 8ES-1.25-2.5-36). In the experiment, eight-bolt 4 wide unstiffened connections suffered from non-ductile failure mode by inner bolt rupture and end plate tearing near the tension flange of the beam. Similar observations were made in the finite element simulated responses (not shown) with no plastic hinge formation and development of strain concentrations near the CJP weld leading to very high strain demands on the inner bolts at the tension flange. It is to be noted here that in this study fracture of the connection is not modeled precisely using fracture mechanics based simulation, as an alternative strain and stress demands at all the locations of the connection are compared to evaluate the potential for ductile failure of the connection. Based on the simulation responses it is evident that the finite element simulation model predicts with sound accuracy the experimental responses of interest and are used to develop techniques for enhancing seismic performance of extended end plate connections.

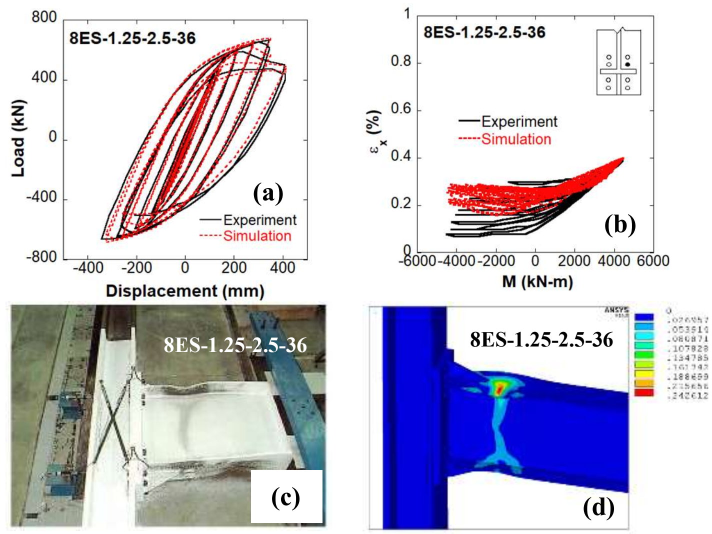

Figure 3. Experimental validation of the finite element model; (a-b) comparison of experimental [21] and simulated (a) moment-rotation responses, (b) bolt strain responses of specimen 8ES-1.25-2.5-36; (c) post-test photograph of specimen 8ES-1.25-2.5-36 [21], (d) von-Mises plastic strain FE prediction of specimen 8ES-1.25-2.5-36 at 6% drift.

EVALUATION OF THE MODIFIED 8-BOLT UNSTIFFENED EXTENDED END PLATE CONNECTION (8EM)

It has been demonstrated through experiments [21] and numerical simulation [12] that the end plate stiffener in eight-bolt stiffened extended end plate connection promotes uniform bolt force distribution and plastic hinge formation away from the CJP welds between end plate and beam flange. However, the stiffener also introduces a stress concentration at the toe of the stiffener which may lead to premature fractures and reduced connection ductility [6, 7, 9, 12]. In addition, the end plate stiffener may increase construction cost because of the fabrication and welding required to attach the stiffener to end plate and beam flanges. Moreover, it has been demonstrated that removal of end plate stiffener and rearrangement of the bolts in a rectangular array of two rows of four bolts at each flange, or four rows of two bolts at each flange, the bolts nearest to the beam flange-to-web intersection resist a larger share of the tensile force leading to unexpected failure of the interior bolts and tearing of end plate [12, 21]. To eliminate the end plate stiffeners (and the associated stress concentration) and to create a favorable load path to promote equal participation among the entire bolt group, an octagonal bolt arrangement as shown in Figure 4 has been proposed in a recent study [12]. This modified connection is referred as 8EM in the discussion. In the octagonal bolt arrangement, the bolts nearest the beam flange-to-web intersection are shifted away, and the bolts farthest from the flange-to-

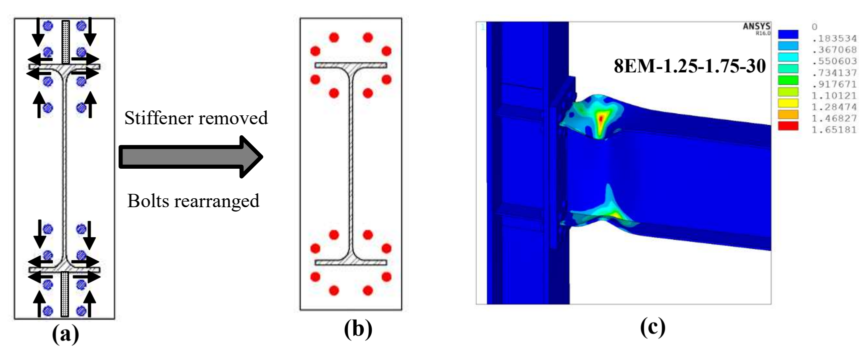

Figure 4. (a-b) Proposed bolt rearrangement in an octagonal pattern (8EM) [12], (c) accumulated equivalent plastic strain contour of 8EM-1.25-1.75-30 connection at 5% drift.

web intersection are shifted closer as shown in Figure 4a. By doing this, beam flange and web forces are uniformly distributed amongst the bolt group. Simulated bolt strain responses of a 8EM connection with W30×99 (W760×147) beam section (ASTM A992) connected to a W14×193 (W360×287) column section (ASTM A992) is shown in Figures 5a,b which indicates that the octagonal bolt pattern is effective in distributing tensile forces uniformly to the connecting bolts and as a result, lowers the strain demands on the bolts located nearest the beam flange-to-web intersection [12]. As shown in Figures 5a,b, strains in the inner (closer to the beam web) and outer bolts located below the flange remained in the elastic range with a gradual decrease in pretension strain with progression of loading cycles. In addition, as illustrated in the Figure 5c strain concentrations at the weld toe remain low throughout the loading history. The plastic hinge formed in the beam flanges away from the CJP weld (Figure 4c) and the strength degradation was delayed compared to the eight-bolt stiffened (8ES) extended end plate connection (Figure 5d). Thus, it is demonstrated that by removing the end plate stiffener, the associated stress concentration is alleviated and by rearranging the bolts in the octagonal pattern bolt forces are evenly distributed. As a result, the proposed modified connection (8EM-1.25-1.75-30) displayed improved global and local seismic performance compared to that of the eight-bolt stiffened (8ES-1.25-1.75-30) connection [12] and demonstrates the potential as a viable and economical alternative to the AISC prequalified 8ES connection.

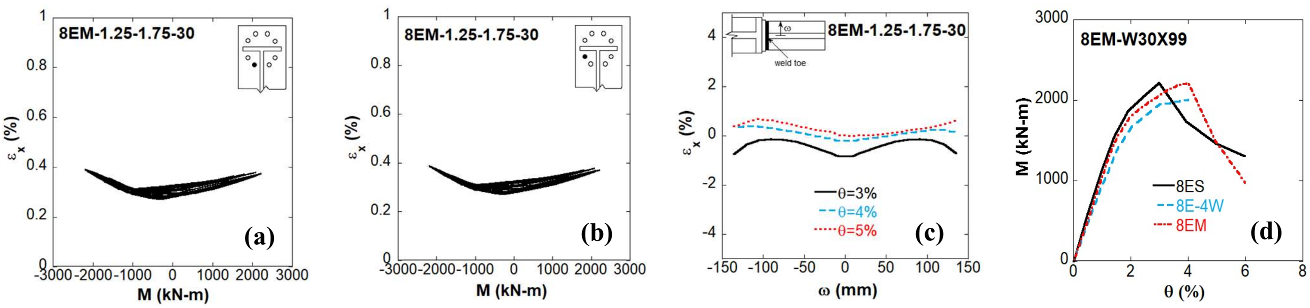

Figure 5. (a) and (b) Simulated bolt strains for 8EM-1.25-1.75-30 connection during loading cycles, (c) simulated axial strain profile at the weld toe across the width of beam bottom flange for 8EM-1.25-1.75-30 connection, (d) moment-rotation envelopes of the extended end plate connections with W30×99 (W760×147) beam section for different bolt arrangements.

FURTHER EVALUATION OF 8EM CONNECTION

The conceptual development of the proposed modified connection (8EM) from Morrison *et al.* [12] was based on analysis responses from a W30×99 (W760×147) beam and a W14×193 (W360×287) column and due to limitation of resources the effect of member size was not explored. It has been demonstrated that welded connections with heavier and deeper beam sections may experience more severe strain concentrations and as a result reduced ductility during seismic loading [22-23]. Therefore, in this study the 8EM is further investigated for two connections involving larger members. One connection evaluated includes a W30×148 (W760×220) beam and a W14×257 (W360×382) column section referred to as 8EM-1.5-1.875-30. The column panel zone was reinforced with 25.4 mm continuity plates and 25.4 mm doubler plate to prevent excessive shear distortions. Another connection with a W36×170 (W920×253) beam and a W14×257 (W360×382) column section referred to as 8EM-1.5-1.875-36 is numerically evaluated. This connection was also reinforced with doubler plate. The member lengths were kept the same as used in studies by Sumner *et al.* [21] and Morrison *et al.* [12]. The beam had lateral supports at a distance of 1.25 m, 2.46 m and 5.72 m from the column centerline. The loading point at the free end of the the beam was located at a distance of 6.13 m from the centerline of the column. The end plate thickness was selected by satisfying the shear strength

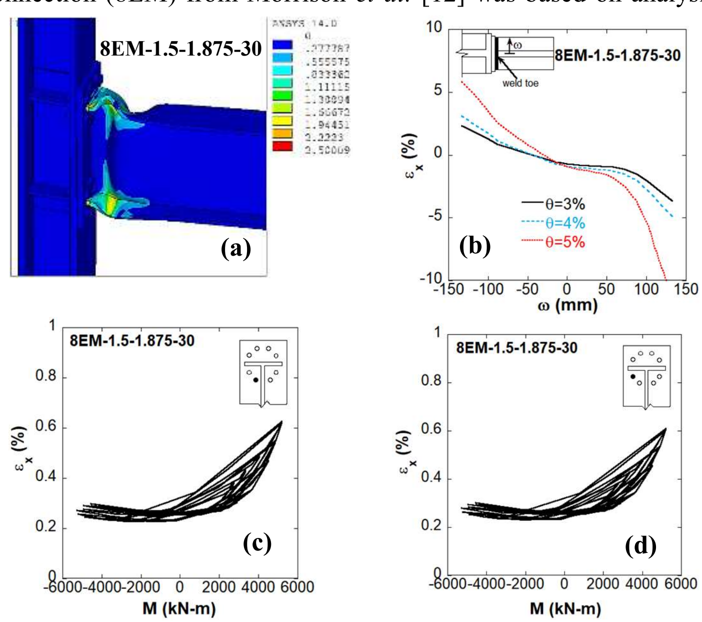

Figure 6. Simulated cyclic response of 8EM-1.5-1.875-30 connection. (a) Accumulated equivalent plastic strain contour, (b) axial strain profile at the weld toe across the width of the beam flange at 6% drift; (c-d) bolt strains.

requirements for the extended portion of the end plate using equations from the ANSI/AISC 358 standard [3]. It is noted that this process was followed in Morrison *et al.* [12] during the conceptual development of the 8EM connection on the W30×99 beam. Based on the uniform distribution of bolt force provided by the 8EM connection each bolt was designed according to the AISC LRFD specifications [16] to resist an equal share of the tensile force component of the expected maximum moment couple at the column face. In both connections the beam and column material were chosen as ASTM A992 and the end plate material was modeled as ASTM A36. Design equations [3, 14] required an end plate thickness of 47.625 mm which was bolted to the column flange with 38.1 mm diameter A490 bolts for both assemblies. The bolts were given a pretension load of 658 kN as specified in the AISC LRFD specification. The connections were analyzed under the simulated seismic loading shown in Figure 2. The accumulated equivalent plastic strain contour and axial strain profile at the weld toe for the 8EM-1.5-1.875-30 connection is shown in Figures 6a and 6b, respectively. The connection exhibited beam flange and web local buckling resulting in plastic hinge formation approximately 150 mm away from the beam flange CJP welds. However, the location of the plastic hinge led to large strain demands at the beam flange-to-end plate CJP welds as demonstrated in Figure 6b. It is observed that tensile strains were approximately 5% during loading cycles at 4% rotation and approached 10% for loading cycles at 5% rotation. Similar observations were made for 8EM-1.5-1.875-36 connection andd hence, not shown here.

SEISMIC PERFORMANCE ENHANCEMENT OF 8EM CONNECTIONS THROUGH HEAT TREATMENT

The large strain demands for larger beam 8EM connections which may cause premature fractures in the weld heat affected zone (HAZ), motivated the use of a recently developed technique [24] to lower strain demands in the beam flange welds of moment connections. This technique reduces material strength at selective regions of beam flanges (heat-treated beam section or HBS) and promotes formation of plastic hinge in those regions away from the beam flange weld. Material strength reduction is achieved through heat-treatment (annealing) of the beam flanges as shown in Figure 7a (areas highlighted in red). The temperature-time history used to heat-treat the beam flanges is shown in Figure 7b and the resulting strength reduction of the A992 steel is shown in Figure 7c.

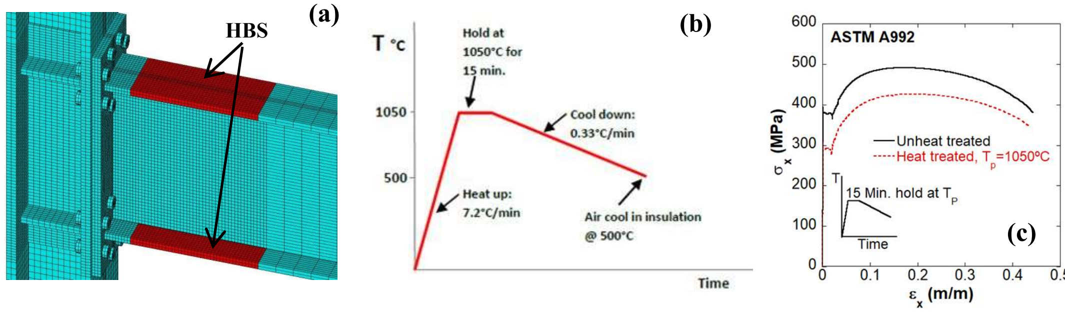

Figure 7. (a-b) HBS applied to modified extended end plate connection for seismic performance enhancement: (a) FE mesh for 8EMH connection, (b) temperature-time history applied to HBS; (c)monotonic stress-strain response of A992 and heat-treated A992 steel [13].

This weakening mechanism of beam flanges is similar to reduced beam section (RBS) other than not sacrificing the elastic stiffness of the connection. During cycling loading, large displacements are accommodated by yielding and local buckling at the heat-treated beam section (HBS) which in turn reduces the inelastic strain demands at the beam flange weld. In the simulation, Chaboche [19] model parameters were determined by simulating stable hysteresis loops from cyclic strain-controlled experiments performed on heat-treated ASTM A992 steel [13]. It is observed that the cyclic stress response of heat-treated ASTM A992 steel stabilizes very quickly (not shown) and hence, the stabilized hysteresis response was used to calibrate the kinematic hardening parameters, and isotropic hardening was not considered. The nonlinear kinematic hardening parameters for the heat-treated ASTM A992 steel used in this study are listed in Table 1.

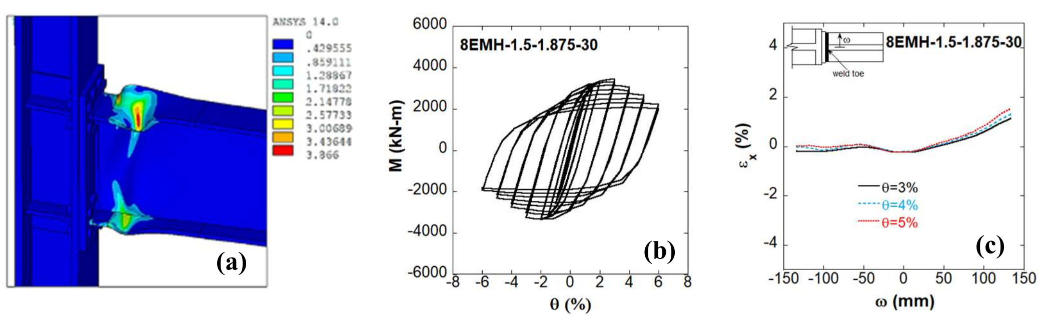

Figure 8. Simulated cyclic response of 8EMH-1.5-1.875-30 connection; (a) accumulated equivalent plastic strain contour, (b) moment rotation response up to 6% interstory drift angle, (c) axial strain profile along beam flange-to-end plate CJP weld toe.

Subsequently the 8EM-1.5-1.875-30 connection modified with HBS were analyzed under the SAC simulated seismic loading. This connection has been referred by 8EMH. The equivalent plastic strain contours along with the moment-rotation responses of 8EMH-1.5-1.875-30 connection are shown in Figures 8a and 8b, respectively. For this connection, wide hysteresis loops and strength degradation initiation after loading cycles at 3% rotation are observed. By comparing Figure 6a to Figure 8a, it can be noted that the plastic hinge is relocated to the HBS region and by doing so, the strain demands at the beam flange-to-end plate CJP welds are reduced significantly as can be observed by comparing Fig. 6b to Fig. 8c. Simulated bolt strains of 8EM-1.5-1.875-30 connection are shown in Figures 9(a-b), where it can be observed that bolt strains are uniformly distributed and magnitudes are reduced with incorporation of the HBS, (compare Figures. 6(c-d) and 9(a-b)). Similar observations were also made for and 8EM-1.5-1.875-36 connection. A comparison of the moment-rotation envelopes of the 8ES and 8EM connections in Figure 5d shows that the strength degradation in 8EM connection was delayed to be initiated at 4% drift, whereas that in 8ES connection was initiated at 3%. However, as the heat treatment was added to the 8EM connection in order to achieve the plastic hinge relocation, strength degradation in the modified 8EMH connection is not similarly delayed (Figure 15c). In addition, the strength degradation rate was rapid once initiated.

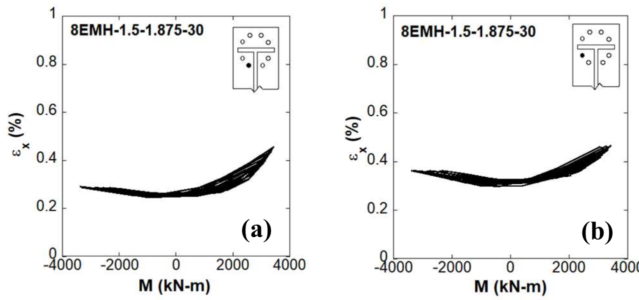

Figure 9. Simulated bolt strains of 8EMH-1.5-1.875-30 connection.

FURTHER SEISMIC PERFORMANCE ENHANCEMENT OF 8EMH CONNECTION

Analysis of the simulated responses of the 8EMH connection demonstrated that the strength degradation of the connection was triggered by beam web local buckling followed by beam flange local buckling resulting in beam lateral torsional buckling. This mechanism is demonstrated for an 8EMH connection in Figure 10, where a cross section at the plastic hinge region of the beam is plotted after loading cycles at 3% and 4% rotation. It is noticed that the beam web started to buckle during the first cycle of 3% rotation (Figure 10a), however no strength degradation was observed at this point of the load history (Figure 10b). During the second cycle of 3% rotation, the beam web started to twist which initiated beam lateral-torsional buckling and in turn led to connection strength degradation (Figure 10b). As the rotation amplitude was further increased, the lateral torsional buckling became more pronounced and strength degradation increased significantly (Figure 10c). Similar observations have been made in other studies [24-26]. Since lateral torsional buckling of the 8EMH

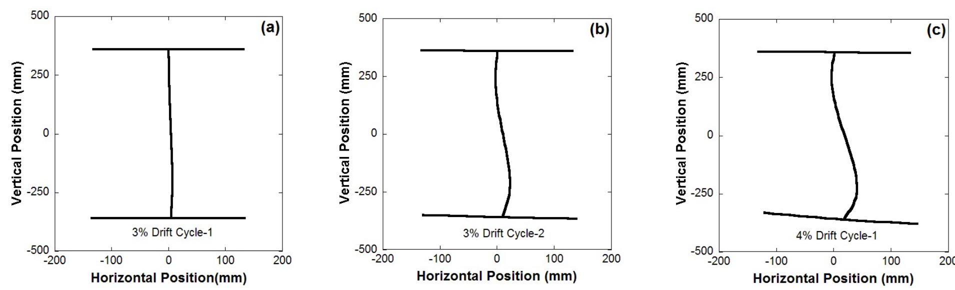

Figure 10. Local buckling of beam web and flanges at different loading cycles for 8EMH-1.5-1.875-30 connection.

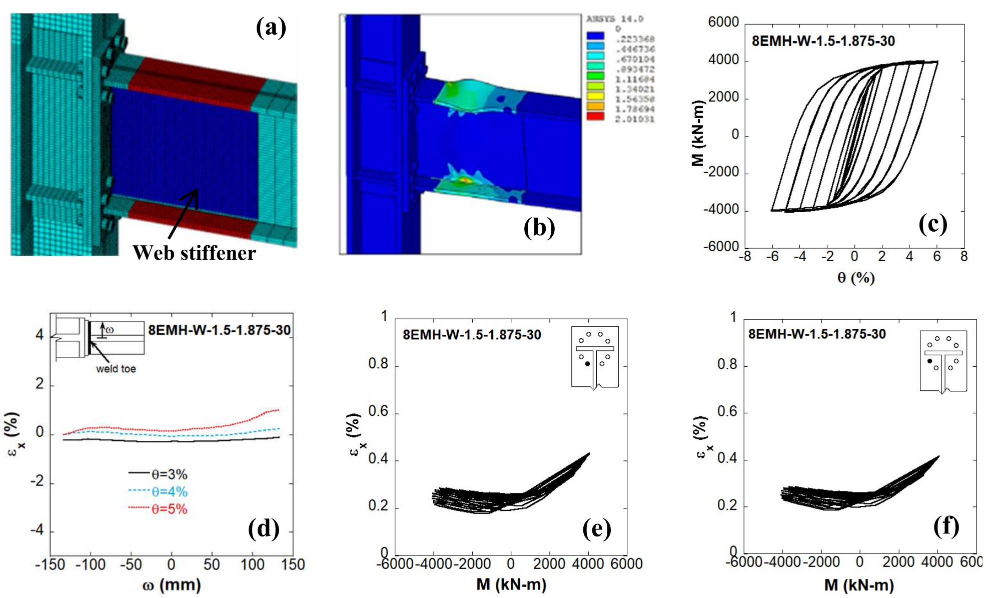

Figure 11. (a) FE mesh of modified extended end plate connection with heat-treatment and web reinforcement, (b) accumulated equivalent plastic strain contour,(c) moment-rotation hysteresis response, (d) axial strain profile at the weld toe across the width of beam bottom flange, and (e-f) bolt strains of 8EMH-W-1.5-1.875-30 connection.

connection was initiated by beam web local buckling, *web reinforcement* was incorporated to delay the initiation of web buckling and thereby delay the strength degradation as well as lateral torsional buckling of the connection. The web reinforced connections are referred by 8EMH-W where 6.35 mm thick plates were attached to the web and end plate with full contact on each side of the beam web (total plate thickness, t_w = 12.7 mm) extending up to the end of the HBS region as shown in Figure 11a. Analysis results of 8EMH-W connection in Figures 11b-c show this connection's potetial in delaying the onset of buckling and strength degradation. No noticeable strength degradation was observed up to 6% rotation, a significantly enhanced performacne compared to other connections as observed in Figure 11c. As the plastic hinge formed in the HBS region, the axial strains at the weld toe remained low throughout the loading history (see Figure 11d).

Moreover, the connecting bolts are equally effective in resisting the beam flange and web forces because of the octagonal bolt arrangement as shown in Figures 11e-f. Excellent seismic performace of this modified connection may increase its potential for use in earthquake prone areas, hence additional parametric studies on 8EMH-W connection are performed. Analyses were performed on 8EMH-W-1.5-1.875-30 connection to study the effect of total web reinforcement plate thickness (t_w) used on both sides of the beam web and it is obsereved that with increase in the plate thickness, the strength of the connection increases until t_w = 12.7 mm (Figure 12a) and the plastic hinge always formed in the HBS (not shown). Also, the connection strength degradation always starts at 5% rotation, and rate of strength degradation decreases with increase in plate thickness. At 6% rotation, the connection's strength decreased by 6, 4 and 1% with total plate thicknesses (t_w) 6.35, 9.525 and 12.7 mm, respectively. On the other hand, when web reinforcement plate thickness increases to 19.05 mm, not much increase in strength is observed, but the strength degradation rate drops sharply after initiation at 5% rotation. In addition, with t_w = 19.05 mm, high strain demand was observed near the CJP weld as shown in Figure 12b. Therefore, for 8EMH-W-1.5-1.875-30 connection, the optimum web reinforcement plate thickness seems to be 12.7 mm. Similar analyses were performed for 8EMH-W connections with W30×99 (W760×147) and W36×170 (W920×253) beam sections, and it was found that the effective web reinforcement plate thickness with these two beams also is 12.7 mm. Based on the simulated responses of 8EMH-W connections with W30×99 (W760×147), W30×148 (W760×220) and W36×170 (W920×253) beam sections, the hypothesis made is that the total web reinforcement plate thickness should be less than the thickness of the beam web. Further analyses will be required for different beam sizes to confirm this hypothesis and develop design gudielines for web reinforcement plate thickness. A comparison of the moment-rotation envelopes of the 8ES, 8EM, 8EMH and 8EMH-W connections with W30×148 (W760×220), W36×170 (W920×253) and W30×99 (W760×147) beam sections are shown in Figs. 15a-c, respectively. From these figures, it is evident that 8EMH-W connection shows a marked improvement compared to the 8ES and 8EMH connections in terms of plastic hinge formation and strength degradation. Based on these results, it is apparent that the proposed design modifications (octagonal bolt arrangement, heat treatment and web reinforcement) for eight bolt extended end plate connections can significantly improve the seismic resilience when compared to the prequalified stiffened eight-bolt extended end plate connection (8ES). Note that according to ANSI/AISC 341 [14], the plastic hinge regions are considered as protected zones and welding is not allowed in these regions. However, Morrison and Hassan [17] have successfully implemented web reinforcement concept for a WUF-W (welded unreinforced flange welded web) HBS connection by welding a steel plate to the beam web in the expected plastic hinge region or protected zone. Finally, it is analytically evaluated if a single plate is attached to one side of the beam web rather than two plates on two sides as presented above, will there be any detrimental effect on the performance enhancement. Hence, an analysis of the 8EMH-W-1.5-1.875-30 connection with a single web reinforcing plate of 12.7 mm thickness attached to the beam web. The results show that no detrimental effect is oberved by attaching web reinformcement plate unsymmetrically on one side of the web (not shown).

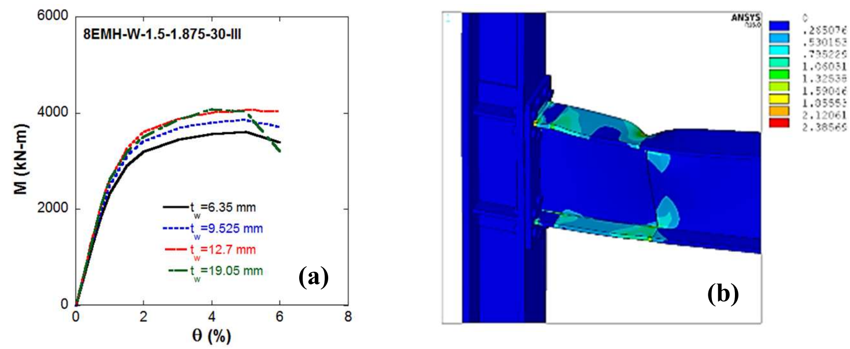

Figure 12. (a) Moment-rotation envelopes of 8EMH-W-1.5-1.875-30 connection for different thicknesses of web reinforcement plates, (b) accumulated equivalent plastic strain contour plot showing formation of plastic hinge at the end of HBS of 8EMH-W-1.5-1.875-30 connection at 5% drift.

SEISMIC PERFORMANCE ENHANCEMENT OF 8EM CONNECTIONS THROUGH EXTENDED SHEAR TAB

Although the proposed modified EEP connection with heat treatment and web reinforcement demonstrated significant enhancement of the seismic resilience of the eight-bolt extended end-plate connection, the heat treatment and web reinforcement attachment increase the fabrication effort and time in addition to increase in construction cost. Hence, as a design alternative to the proposed modified connection, the 8EM connection is investigated with a heavy extended shear tab between the end plate and the beam web. Heavy extended shear tab has been used in the seismic testing of welded unreinforced flange welded web moment resisting connections performed by Ricles *et al.* [27] where it was demonstrated that heavy extended shear tab relocates plastic hinge to form away from the weld toe and lead to ductile failure of the connection without any detrimental effect on the performance. Ricles *et al.* [27] used a 32 mm thick shear tab extending 254 mm from the face of the column for a moment connection consisting of a W36×150 beam and a W14×311 column. The shear tab was connected to the column flange by complete joint penetration groove weld. Moreover, the edges of the shear tab were continuously fillet welded to the beam web. Hence, based on the responses observed in the study by Ricles *et al.* [27], this study investigates the seismic performance of the EEP connection with octagonal bolt arrangement and an extended shear tab which is referred as 8EMS connection (Figure 13a). In the finite element models, ASTM A572 Gr. 50 shear tab is connected to the end plate by CJP weld and fillet welded around the edges to the beam web. The shear tab is placed only on one side of the beam web and considered to be in full contact with the beam web and end plate. In other words, the shear tab increased the beam web thickness for the width of the shear tab.

First, the 8EMS connection is analyzed under simulated seismic loading by considering W30×148 beam section (referred as 8EMS-1.5-1.875-30) with the same width and thickness of shear tab as used by Ricles *et al.* [27] to investigate the feasibility of using an extended shear tab with the modified 8EM connection. This connection has the same configurations as the 8EM-1.5-1.875-30 connection other than the introduction of an extended shear tab between the end plate and the beam web. The accumulated equivalent plastic strain contour of the connection is shown in Figure 13b where it is observed that the shear tab relocates the plastic hinge at the end of the shear tab and as a result the strain demand at the weld toe remained below 1% as shown in Figure 13d. The moment-rotation hysteresis response of this connection (Figure 13c) demonstrates that the connection can sustain 4% rotation with very negligible strength degradation (less than 5%) which initiated at the 2nd cycle of 4% rotation. In addition, bolt forces are observed to be relatively uniform as demonstrated in Figures 13e and 13f which show the inner and outer bolt strains for bolts below the top flange for the 8EMS-1.5-1.875-30 connection. Therefore, the simulated responses demonstrate that the extended shear tab can effectively relocate the plastic hinge away from the weld toe and reduce the high strain demands at the weld toe of the 8EM connection and satisfy the 4% interstory drift angle criteria of ANSI/AISC 341 [14] for special moment frame.

Hence, further analyses are performed on the 8EMS-1.5-1.875-30 connection by varying the shear tab width between 127-254 mm and thickness between 6.35-25.4 mm to investigate the influence of these parameters on the strength degradation of the connection and the strain demands at the beam flange CJP weld. Figs. 14a-b shows the moment-rotation envelopes and axial strain profiles at the weld toe of 8EMS-1.5-1.875-30 connection for different thicknesses of a 254 mm wide shear tab. It is observed that the strength of the connection is insensitive to the thickness of the shear tab. However, there is decrease in the post-peak strength degradation rate with increase in shear tab thickness. On the other hand, the weld strain demands keep decreasing with increase in the thickness of the shear tab upto a shear tab thickness equal to the beam web thickness, after which the weld strain demands are comparable even though the thickness of the shear tab is increased. As a result, further analyses are performed by considering a thickness of the shear tab at least equal to or more than the thickness of the beam web which is taken as 15.875 mm for 8EMS-1.5-1.875-30 connection. Analyses results of the 8EMS connection with 15.875 mm thick shear

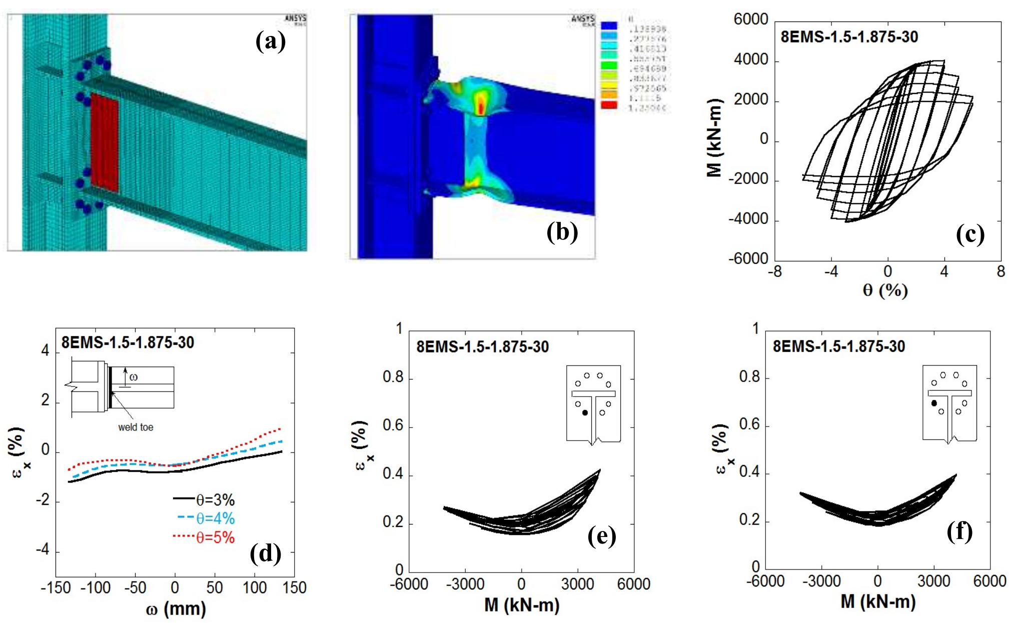

Figure 13. (a) FE mesh of modified extended end plate connection with extended shear tab, (b) accumulated equivalent plastic strain contour,(c) moment-rotation hysteresis response, (d) axial strain profile at the weld toe across the width of beam bottom flange, and (e-f) bolt strains of 8EMS-1.5-1.875-30 connection.

tab for three different widths are presented in Figures 14c-d, where moment-rotation envelopes and axial strain profiles at the weld toe are plotted for different widths of a 15.875 mm thick shear tab. It is noted that there is a slight increase in the capacity of the connection and decrease in the post-peak strength degradation rate with increase in the shear tab width. On the other hand, the strain demands at the weld toe decreases significantly with increase in the shear tab width which is as expected since with increase in the shear tab width, the location of plastic hinge shifts away from the weld toe. Considering the strength degradation and weld toe strain demands, it is noted that a shear tab width of 254 mm produces the most desirable results for the connection. Hence, based on the responses of the 8EMS-1.5-1.875-30 connection, it is hypothesized that for 8EMS connection, the extended shear tab must be 254 mm wide and must have a thickness either equal to or more than the thickness of the beam web in order to sustain 4% interstory drift angle with low strain demands at the beam flange CJP welds. Two more connections are analyzed to test the hypothesis with beam sections W36×170 and W30×99 with 254 mm wide shear tab with a thickness equal to the beam web and similar observations are made.

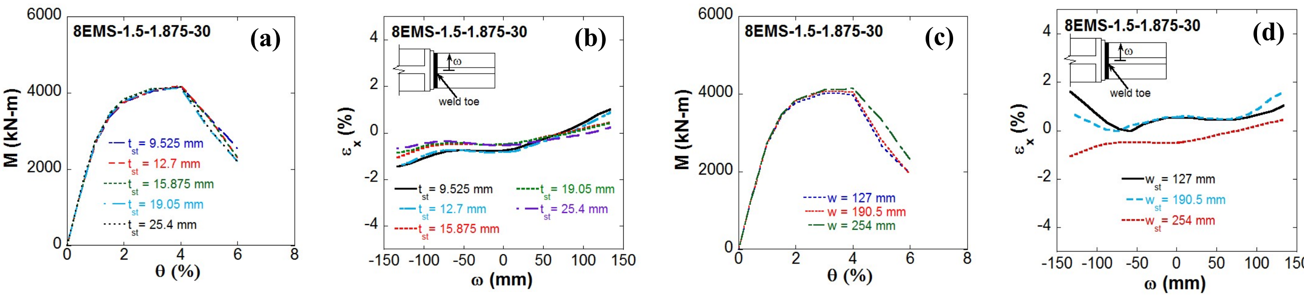

Figure 14. (a-b) Simulated cyclic response of 8EMS-1.5-1.875-30 connection for a 254 mm wide shear tab with different thicknesses: (a) momen-rotation envelopes, and (b) axial strain profile at the weld toe across the width of beam top flange; (c-d) simulated cyclic response of 8EMS-1.5-1.875-30 connection for a 15.875 mm thick shear tab with diferent widths: (c) momen-rotation envelopes, and (d) axial strain profile at the weld toe across the width of beam top flange.

The moment-rotation envelopes of 8EMS connection with W30×14, W36×170 and W30×99 beam sections are compared to those of the other modified design of the connection (i.e 8ES, 8EM, 8EMH and 8EMH-W) presented in Figures 15a-c. It is observed that the peak strength of the 8EMS connection is comparable to 8EMH-W connection other than the strength degradation which initiates earlier than the 8EMH-W connection. However, the strength degradation is delayed when compared to 8EM, 8EMH and 8ES connections and the rate of strength degradation is slower than 8EM and 8ES connections. Overall, 8EMS connection shows improved performance when compared to 8EM, 8EMH and 8ES connections in terms of strength degradation and strain demands at the beam flange CJP weld toe (Figure 15d). 8EMH-W connection obviously performs better than 8EMS connection in terms of strength degradation and energy dissipation; nevertheless, 8EMS connection shows potential for an economic alternative to 8EMH-W connection by satisfying the 4% ANSI/AISC 341 [14] qualifying criteria for special moment frames. Hence, the proposed design modifications of the EEP connection with octagonal bolt arrangement and a heavy extended shear tab are effective in sustaining the seismic demands of a moment resisting connection by delaying the onset of buckling with minimal strain demands at the beam flange CJP weld. Note that the 8EMS connection proposed in this study has not been experimentally evaluated yet due to limited resources and needs experimental verification before its implementation and design development.

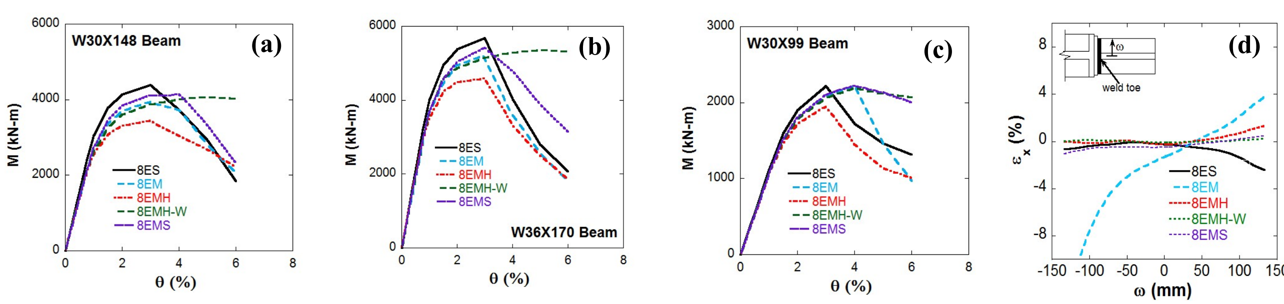

Figure 15. Moment-rotation envelopes of extended end plate connections with different design options. (a) W30×148 (W760×220) beam section, (b) W36×170 (W920×253) beam section, and (c) W30×99 (W760×147) beam section. (d) axial strain profile at weld toe.

CONCLUSIONS

This study analytically investigated the seismic performance of various eight-bolt extended end plate moment connections, started with the eight-bolt stiffened extended end plate (8ES) connection, which is currently prequalified by ANSI/AISC 358 [3]. Based on the strengths and drawbacks of the 8ES connections observed, various modifications to the 8ES connections were progressively introduced and analyzed. For analysis, a detailed finite element simulation model in ANSYS was developed incorporating time-independent nonlinear kinematic hardening model of Chaboche [19] and validated against experimental responses of four EEP moment connections. The FE simulation model included interactions between bolts, end plate and column flange through contact and target elements. Initial bolt tension was modeled using the pretension element. Such detailed nonlinear finite element modeling enabled accurate simulation of both local responses (bolt strain and local buckling) and global responses (connection strength, stiffness and moment-rotation hysteresis response) with very good accuracy. This robust, experimentally verified simulation modeling scheme was then implemented to gradually evaluate various seismic performance modification techniques for EEP connections.

First modification to the 8ES connection evaluated was removal of the end plate stiffener and change the bolt pattern to octagonal arrangement (see Figure 4) as proposed by Morrison *et al*. [12]. This connection was referred by 8EM, which demonstrated reduced stress and strain concentrations at beam flanges (compared to AISC prequalified 8ES connection), even distribution of flange forces to the connecting bolts, and finally delayed and reduced rate of strength degredation. Overall, the 8EM connection improved the global and local seismic performance of the connections with W30×99 (W760×147) beam as also was demonstrated by Morrison *et al*. [12]. However, as the 8EM connection size was increased to W30×148 (W760×220) beam and W14×257 (W360×382) column or W36×170 (W920×253) beam and W14×257 (W360×382) column, large strain demands are placed on the beam flange-to-end plate CJP welds which may deteriorate their seismic performances. It was also observed that the initiation of strength degradation was delayed compared to the 8ES connection, however, once initiated, the strength degradation rate was rapid. In order to enhance seismic performance of larger 8EM connections, this study next implemented a recently developed plastic hinge relocation technique, which is known as heat-treated beam section (HBS) (Figure 7) [24]. This connection is referred by 8EMH, which successfully relocated the plastic hinges away from the end plate CJP welds (Figure 8) and consequently lowered the strain demands at the welded joint. The 8EMH connection, however, was observed to initiate strength degradation during the 2nd cycle of the 3% interstory drift due to the mechanisms initiated by the beam web buckling followed by the beam flange and lateral torsional buckling (Figure 10). To improve buckling resistance of the 8EMH connection, three different web reinforcement techniques were evaluated. The technique that reinforces the web of the plastic hinge region by attaching plate(s) directly to the web extending from the HBS external edge to the beam end plate (referred by 8EMH-W connection), as shown in Figure 11a, performs excellent in resisting seismic loading without any or much strength degradation up to 6% interstory drift for the three connection sizes studied. This connection is experimentally validated which demonstrates the fidelity of the introduced concepts of seismic performance enhancement techniques.

The modified EEP connection (with heat treatment and web reinforcement) demonstrates excellent failure resilience, buckling resistance, and energy dissipation which substantially exceeded the ANSI/AISC 341 qualifying criteria of a moment resisting connection for special moment frames; however, the fabrication and construction of the connection requires additional effort and cost. Hence, in order to economize the connection but still satisfying the 4% interstory drift angle qualifying criteria of ANSI/AISC 341, an alternative connection is analyzed by using the octagonal bolt arrangement with a heavy extended shear tab in between the end plate and beam web (Figure 13a) which is referred as 8EMS connection. The extended shear tab effectively relocated the plastic hinges away from the CJP welded joint in addition to strengthening the beam web in the connection region which helped in delaying the strength degradation. As a result, the 8EMS connection sustained 4% interstory drift angle without much strength degradation and with low strain demand at the CJP welds; nevertheless, the connection loses strength rapidly after reaching the peak strength and hence, is not able to dissipate as much energy as the 8EMH-W connection. It is noted, however, that the proposed 8EMS connection will need experimental verification before its implementation.

The seismic performance of the two types of modified EEP connection proposed in this study demonstrates improved performances compared to the seismic response of the eight-bolt stiffened extended end plate (8ES) connection, which is currently prequalified by ANSI/AISC 358. The 8EMH-W connection showed significant improvement over the 8ES connection in terms of fatigue failure resilience, buckling resistance, and energy dissipation which can sustain upto 6% interstory drift angle without much strength degradation, whereas the 8EMS connection shows slight improvement over the 8ES connection and satisfies the ANSI/AISC 341 qualifying criteria. However, both the proposed connections eliminate the necessity of the end-plate stiffener which attenuates the stress concentration on the beam flanges. Hence, the modified extended end plate connections developed in this study demonstrate potential to be used as viable alternatives to the AISC prequalified 8ES connection. However, a validated design methodology needs to be established for practical use of these modified EEP connections. This study serves as the starting point for such design development and future testing and analyses should be tailored towards developing design procedures for these connections addressing several aspects of the connection, in particular, the limits of beam and column size including beam flange thickness, member depth, limiting dimensions of the octagonal bolt arrangement, yield line parameters and attachment of web reinforcement plates and extended shear tab.

REFERENCES

[1] D'Aniello, M., Tartaglia, R., Costanzo, S., and Landolfo, R. (2017). "Seismic design of extended stiffened end-plate joints in the framework of Eurocodes." *Journal of Constructional Steel Research*, 128, 512–27.
[2] Murray, T.M., and Sumner, E.A. (2003). *AISC design guide series 4, Extended end-plate moment connections*. American Institute of Steel Construction, Chicago, IL.
[3] ANSI/AISC 358 (2010). *Prequalified Connections for special and intermediate steel moment frames for Seismic Applications*. American Institute of Steel Construction, Chicago, IL.
[4] Ghobarah, A., Osman, A., and Korol, R.M. (1990). "Behaviour of extended end-plate connections under cyclic loading." *Engineering Structures*, 12(1), 15-27.
[5] Adey, B.T., Grondin, G.Y., and Cheng, J.J.R. (2000). "Cyclic loading of end plate moment connections." *Canadian Journal of Civil Engineering*, 27, 683-701.
[6] Guo, B., Gu, Q., and Liu F. (2006). "Experimental behavior of stiffened and unstiffened end-plate connections under cyclic loading." *Journal of Structural Engineering*, 132(9), 1352-1357.
[7] Shi, G., Shi, Y., and Wang, Y. (2007). "Behaviour of end-plate moment connections under earthquake loading." *Engineering Structures*, 29(5), 703-716.
[8] Eatherton, M., Toellner, B.,Watkins, C., Abbas, E. (2013). *The effect of powder actuated fasteners on the seismic performance of protected zones in steel moment frames*. Virginia Tech SEM Report Series, Report No. CE/VPI-ST-13/05.
[9] FEMA-355B (2000). *State of the art report on welding and inspection*. Prepared by the SAC Joint Venture for the Federal Emergency Management Agency, Washington, DC.
[10] SAC/BD-00/06 (2000). Round robin testing of ultrasonic testing technicians. by Shaw, R.E., Jr.
[11] Quayyum, S. (2014). Advanced finite element analyses of moment resisting connections for improving seismic performance and exploring effects of residual stress and fire damage. Doctoral Dissertation, North Carolina State University, Raleigh, NC, 2014.
[12] Morrison, M.L., Quayyum, S., and Hassan, T. (2017). "Performance enhancement of eight bolt extended end plate moment connections under simulated seismic loading." *Engineering Structures*, 151, 444-458.
[13] Morrison, M.L. (2015). Innovative seismic performance enhancement techniques for steel building moment resisting connections. Doctoral Dissertation, North Carolina State University, Raleigh, NC.
[14] ANSI/AISC 341 (2010). *Seismic provisions for structural steel buildings*. American Institute of Steel Construction, Chicago, IL.
[15] SAC/BD-97/02 (1997). *Protocol for fabrication, inspection, testing and documentation of beam-column connection tests and other experimental specimens*. by Clark, P., Frank, K., Krawinkler, H., and Shaw, R.
[16] AISC (2005). *Steel construction manual, 13th Ed*. American Institute of Steel Construction Chicago, IL.
[17] Morrison, M.L., and Hassan, T. (2016). "Resilient welded steel moment connections by enhancing beam buckling resistance." *Journal of Constructional Steel Research*, 127, 77-91.
[18] Myers, A. (2001). Testing and probabilistic simulation of dutile fracture inititation in structural steel components and weldments. Doctoral Dissertation, Stanford University, Stanford, CA.
[19] *Chaboche, J.L. (1989). "Time-independent constitutive theories for cyclic plasticity."* International Journal of Plasticity, 2(2), *149–188*.
[20] Kaufmann, E.J., Metrovich, B.R., and Pense, A.W. (2001). *Characterization of cyclic inelastic strain behavior on properties of A572 Gr. 50 and A913 Gr. 50 rolled sections*. ATLSS Report No. 01-13, Lehigh University, Bethlehem, PA.
[21] SAC/BD-00/21 (2000). *Cyclic testing of bolted moment end-plate connections*. by Sumner, E.A., Mays, T., and Murray, T.M.
[22] Roeder, C.W., and Foutch, D.A. (1996). "Experimental results for seismic resistance steel moment frame connections." *Journal of Structural Engineering*, 122(6), 581-588.
[23] SAC/BD-98/01 (1998). *Strength and ductility of FR welded-bolted connections*. by El Tawil, S., Mikesell, T., Vidarsson, E., and Kunnath, S.K.
[24] Morrison, M.L., Schweizer, D., and Hassan, T. (2015). "An innovative seismic performance enhancement technique for steel building moment resisting connections." *Journal of Constructional Steel Research*, 109, 34-46.
[25] SAC/BD-00/27 (2000). *Steel moment resisting connections reinforced with cover and flange plates*. by Kim, T., Whittaker, A.S., Bertero, V.V., Gilani, A.S.J., and Takhirov, S.M.
[26] Uang, C.M., and Fan, C.C. (2001). "Cyclic stability criteria for steel moment connections with reduced beam section." *Journal of Structural Engineering*, 127(9), 1021-1027.
[27] Ricles, J.M., Fisher, J.W., Lu, L.W., and Kaufmann, E.J. (2002). "Development of improved welded moment connections for earthquake-resistant design." *Journal of Constructional Steel Research*, 58, 565-604.